Photo-assisted electrocatalytic reduction of CO2: A new strategy for reducing catalytic overpotentials

Article

Supplemental Material

Hartl, F. ORCID: https://orcid.org/0000-0002-7013-5360, Taylor, J. O. and Wang, Y. (2020) Photo-assisted electrocatalytic reduction of CO2: A new strategy for reducing catalytic overpotentials. ChemCatChem, 12 (1). pp. 386-393. ISSN 1867-3899 doi: https://doi.org/10.1002/cctc.201901887 Available at https://centaur.reading.ac.uk/87506/

To link to this article DOI: http://dx.doi.org/10.1002/cctc.201901887

Publisher: Wiley

Photo-assisted Electrocatalytic Reduction of CO_2: A New Strategy for Reducing Catalytic Overpotentials

James O. Taylor[a], Yibo Wang,[a] and František Hartl*[a]

Abstract: Electrochemical and photochemical reduction of CO_2 are both well-established, independent catalytic routes toward producing added-value chemicals. The potential for any cross-reactivity has, however, hardly been explored so far. In this report, we assess a system primarily using spectroelectrochemical monitoring, where photochemistry assists the cathodic activation of precursor complexes [Mn(CO)$_3$(2,2'-bipyridine)Br] and [Mo(CO)$_4$(6,6'-dimethyl-2,2'-bipyridine)] to lower the catalytic overpotential needed to trigger the electrocatalytic reduction of CO_2 to CO. Following the complete initial 1e$^-$ reduction of the parent complexes, the key photochemical cleavage of the Mn–Mn and Mo–CO bonds in the reduction products, [Mn(CO)$_3$(2,2'-bipyridine)]$_2$ and [Mo(CO)$_4$(6,6'-dimethyl-2,2'-bipyridine)]$^{\bullet-}$, respectively, generates the 2e$^-$-reduced, 5-coordinate catalysts, [Mn(CO)$_3$(2,2'-bipyridine)]$^-$ and [Mo(CO)$_3$(6,6'-dimethyl-2,2'-bipyridine)]$^{2-}$ appreciably closer to the initial cathodic wave R1. Experiments under CO_2 confirm the activity of both electrocatalysts under the photoirradiation with 405-nm and 365-nm light, respectively. This remarkable achievement corresponds to a *ca.* 500 mV positive shift of the catalytic onset compared to the exclusive standard electrocatalytic activation.

DOI: 10.1002/anie.2016XXXXX

---

[a] J.O. Taylor, Y. Wang, Prof. Dr. F. Hartl
Department of Chemistry
University of Reading
Whiteknights, Reading, RG6 6AD
United Kingdom
E-mail: f.hartl@reading.ac.uk

Experimental Procedures

Materials

Tetrahydrofuran (THF, Fisher) was freshly distilled from sodium/benzophenone (soluble purple ketyl radicals). Prior to use, the solvent was bubbled with dry argon (BOC, 99.9%) on a frit. The supporting electrolyte, tetrabutylammonium hexafluorophosphate (TBAH, >99.8%, Acros-Organics) was recrystallized twice from hot ethanol and then dried under vacuum. The supporting electrolyte was dried prior to use once more at 120 °C for 12 h. All electrochemical measurements were conducted under an atmosphere of dry argon, or CO_2 (BOC, 99.9%), using standard Schlenk techniques. Prior to electrocatalytic experiments, solutions were saturated with CO_2 by bubbling on a frit at the atmospheric pressure. [Mn(CO)$_3$(2,2'-bipyridine)Br] (**1**) (ref. [1]), [Mn(CO)$_3$(2,2'-bipyridine)(OTf)] (ref [2]) and [Mo(CO)$_4$(6,6'-dimethyl-2,2'-bipyridine)] (**2**) (ref. [3]) were synthesised in house according to the established literature procedures. ^{1}H NMR spectra were measured on Bruker 400 MHz Nanobay spectrometer. The identity and purity of the studied complexes was confirmed by a combination of IR spectroscopy, ^{1}H NMR spectroscopy and cyclic voltammetry. [Mn(CO)$_3$(2,2'-bipyridine)Br]: IR (THF), v(CO) at 2023, 1934 and 1915 cm^{-1}. [Mn(CO)$_3$(2,2'-bipyridine)(OTf)]: IR (THF), v(CO) at 2043 and 1943 cm^{-1}; ^{1}H NMR (400 MHz, $CDCl_3$) δ 9.28 (2H, d, *J* = 5.2 Hz), 8.16 (4H, m, *J* = 8 Hz), 7.32 (2H, t, *J* = 6 Hz). [Mo(CO)$_4$(6,6'-dimethyl-2,2'-bipyridine)]: IR (THF), v(CO) at 2014, 1899, 1879 and 1836 cm^{-1}; ^{1}H NMR (400 MHz, CD_2Cl_2) δ 7.84 (2H, d, *J* = 7.6 Hz), 7.74 (2H, t, *J* = 7.5 Hz), 7.32 (2H, d, *J* = 7.1 Hz), 2.95 (6H, s).

Methods

Cyclic Voltammetry

Cyclic voltammograms were recorded on a PGSTAT302N potentiostat (Metrohm Autolab) under an atmosphere of dry argon using a standard configuration of an airtight, three-electrode, single-compartment cell. Pt, Au or Cu microdiscs (all *d* = 0.4 mm), polished by a 0.25-μm diamond paste (Kemet), served as the working electrode; the auxiliary and pseudoreference electrodes were made of coiled Pt and Ag wires, respectively, protected by a glass mantle. Ferrocene (Fc) served as the internal potential reference for these measurements and was added just before the ultimate voltammetric scan. The solutions prepared for cyclic voltammetry contained 1 mM analyte and 10^{-1} M TBAH.

Infrared and UV-vis Spectroelectrochemistry

Infrared spectroelectrochemical experiments were performed on a Bruker Vertex 70v FTIR spectrometer, equipped with a DTLaGS detector. UV−vis spectroelectrochemical experiments were conducted on a Scinco S-3100 diode array spectrophotometer. The electrochemical response in the form of a thin-layer cyclic voltammogram (TL-CV) at v = 2 mV s^{-1} was recorded during both IR and UV-vis monitoring of the controlled-potential electrolyses with an EmStat3 potentiostat (PalmSens). The spectroelectrochemical measurements were conducted with an optically transparent thin-layer electrochemical (OTTLE) cell (Spectroelectrochemistry Reading)[4]. The cell was equipped with either a Pt, Au or Cu minigrid working electrode, a Pt minigrid auxiliary electrode, an Ag microwire pseudoreference electrode and CaF_2 optical windows. The solutions prepared for spectroelectrochemistry contained 3 mM analyte and 3×10^{-1} M TBAH.

Photochemistry

In situ irradiation of the masked active cathodic space of the OTTLE cell during the cathodic electrolyses was accomplished using a light-emitting diode (LED) driver (ThorLabs). A 405-nm LED (M405L4) was used for [Mn(CO)$_3$(bipy)Br] and a 365-nm LED (M365L2) for [Mo(CO)$_4$(6,6'-dmbipy)] experiments, both equipped with a collimating lens. The LED was placed in front of the cell window and switched on to a maximum power once the initial 1e$^-$ electrochemical reduction of the parent complex was complete. Samples were irradiated and spectra recorded at 5 min or 10 min intervals, up to a maximum of 45 min total irradiation time; this was sufficient in most cases to convert 60-70% of the starting material to the further reducible photoproduct, as revealed by IR spectral monitoring.

Spectro-Electrochemical Figures

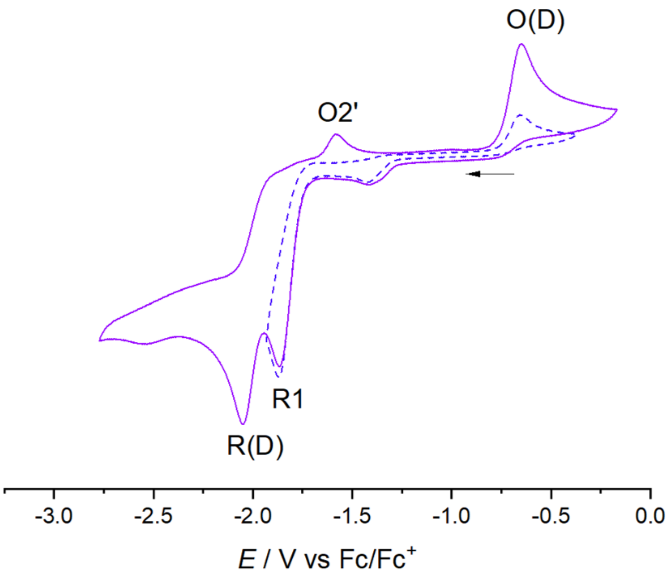

Figure SI-1. Cyclic voltammogram of [Mn(CO)$_3$(bipy)Br]. Conditions: Ar-saturated THF/TBAH, Pt microdisc electrode, *v* = 100 mV s^{-1}, *T* = 298 K. Legend: R1 – reduction of the parent complex; R(D) and O(D) – reduction and oxidation of [Mn(CO)$_3$(bipy)]$_2$; O2' – oxidation of [Mn(CO)$_3$(bipy)]$^-$.

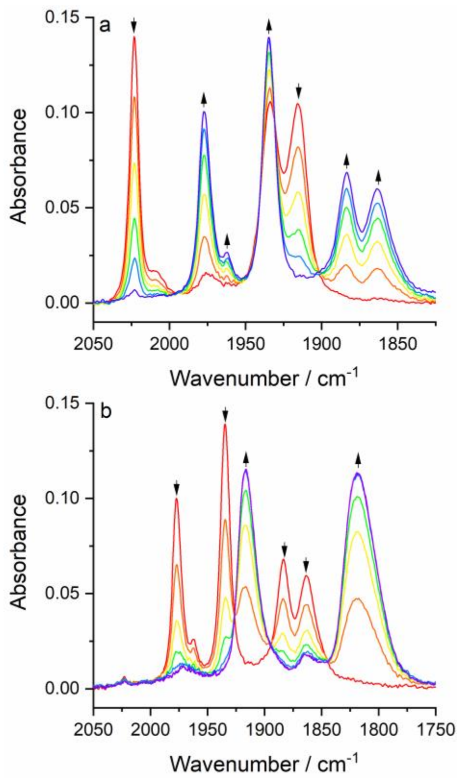

Figure SI-2. IR SEC monitoring of [Mn(CO)$_3$(bipy)Br] during (a) the initial reduction at R1 producing the dimer [Mn(CO)$_3$(bipy)]$_2$, and (b) the subsequent dimer reduction at R(D) to give the 5-coordinate anion [Mn(CO)$_3$(bipy)]$^-$. Conditions: Ar-saturated THF/TBAH, an OTTLE cell (Pt-mesh cathode), *T* = 298 K.

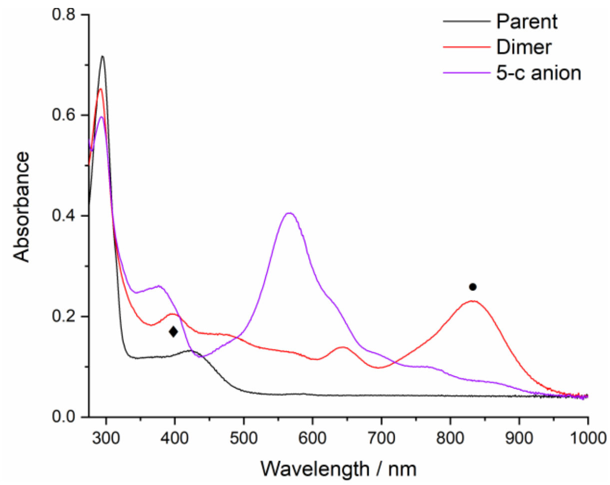

Figure SI-3. UV-vis spectra of parent [Mn(CO)$_3$(bipy)Br] (black), the dimer [Mn(CO)$_3$(bipy)]$_2$ (red) and the 5-coordinate anion, [Mn(CO)$_3$(bipy)]$^-$ (purple). The label ♦ denotes the irradiation wavelength used for the dimer to cleave the Mn–Mn bond; the label ● indicates the optical excitation with no photoreaction observed. Conditions: Ar-saturated THF/TBAH, an OTTLE cell (Pt mesh cathode), *T* = 298 K.

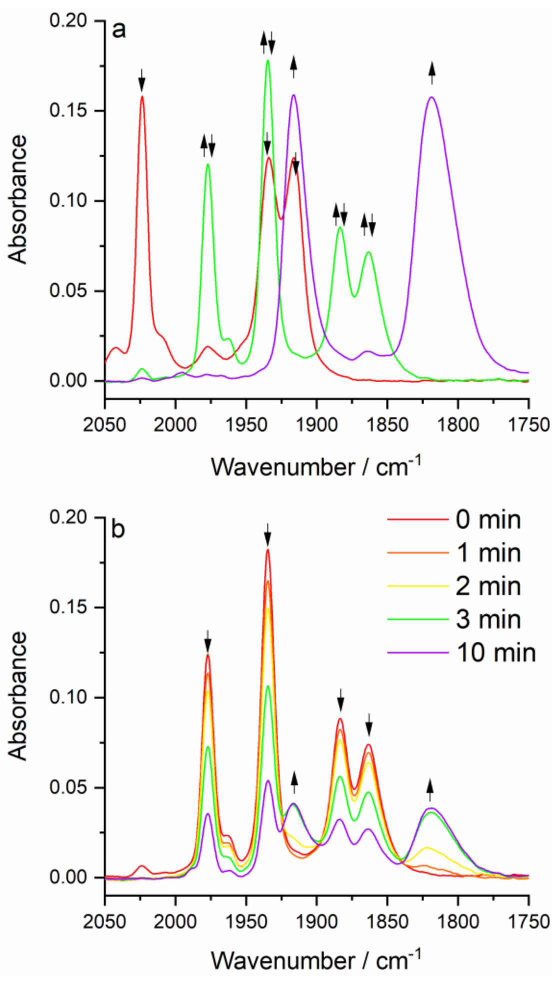

Figure SI-4. IR SEC monitoring of (a) the standard electrochemical reduction of [Mn(CO)$_3$(bipy)Br] (**1**) (↓) to [Mn(CO)$_3$(bipy)]$_2$ (↑↓) at R1, and the dimer to [Mn(CO)$_3$(bipy)]$^-$ (↑) at R(D), and (b) the photo-assisted electrochemical reduction of [Mn(CO)$_3$(bipy)]$_2$ (↓) pre-formed from **1** at R1, to [Mn(CO)$_3$(bipy)]$^-$ (↑) at the same cathodic potential. Conditions: Ar-saturated THF/TBAH containing 5% TFE, an OTTLE cell (Pt mesh cathode), λ_{exc} = 405 nm (irradiation times in minutes), *T* = 298 K.

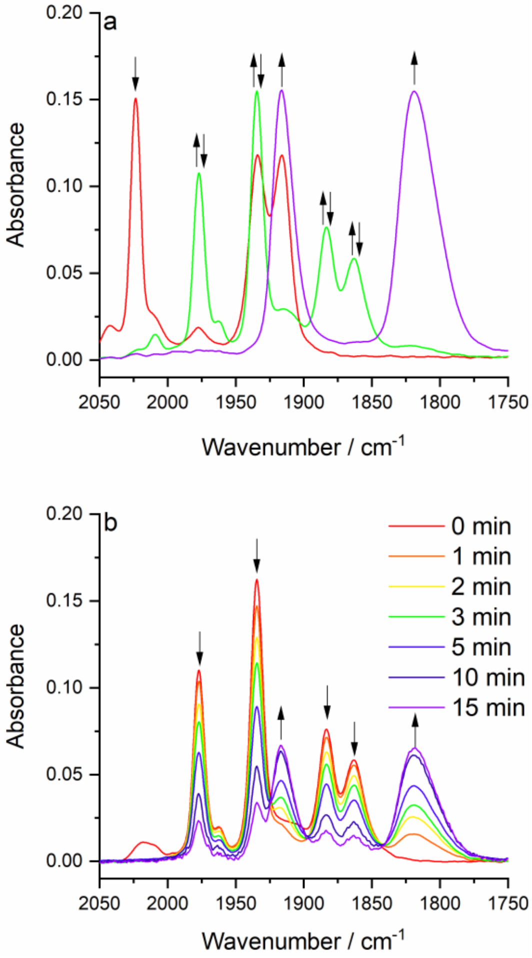

Figure SI-5. IR SEC monitoring of (a) the standard electrochemical reduction of [Mn(CO)$_3$(bipy)Br] (**1**) (↓) to [Mn(CO)$_3$(bipy)]$_2$ (↑↓) at R1, and the dimer to [Mn(CO)$_3$(bipy)]$^-$ (↑) at R(D), and (b) the photo-assisted electrochemical reduction of [Mn(CO)$_3$(bipy)]$_2$ (↓) pre-formed from **1** at R1, to [Mn(CO)$_3$(bipy)]$^-$ (↑) at the same cathodic potential. Conditions: Ar-saturated THF/TBAH containing 5% MeOH, an OTTLE cell (Pt mesh cathode), λ_{exc} = 405 nm (irradiation times in minutes), T = 298 K.

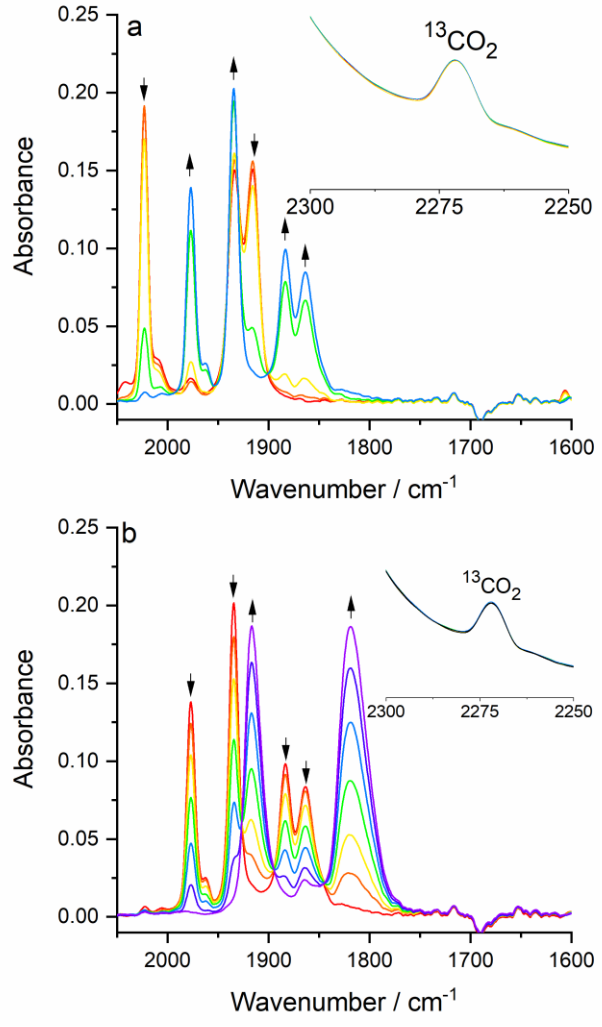

Figure SI-6. IR SEC monitoring of the electrochemical reduction of (a) 1 (↓) at the cathodic wave R1 to $[Mn(CO)_3(bipy)]_2$ (↑), and (b) the dimer (↓) to $[Mn(CO)_3(bipy)]^-$ (↑) at the cathodic wave R(D). Insets: the $^{13}CO_2$ satellite peak used as a reference. Conditions: CO_2-saturated dry THF/TBAH, an OTTLE cell (Pt mesh cathode), T = 298 K. No catalytic activation of CO_2 was observed under these conditions.

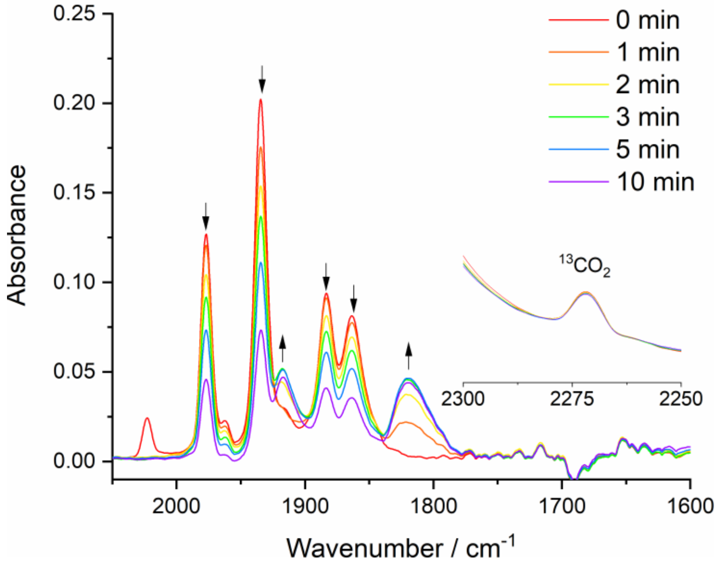

Figure SI-7. IR SEC monitoring of the photo-assisted electrochemical reduction of $[Mn(CO)_3(bipy)]_2$ (↓) pre-formed from **1** at R1, to $[Mn(CO)_3(bipy)]^-$ (↑) at the same cathodic potential. Inset: the $^{13}CO_2$ satellite peak used as a reference. Conditions: CO_2-saturated dry THF/TBAH, an OTTLE cell (Pt mesh cathode), λ_{exc} = 405 nm (irradiation times in minutes), T = 298 K. No catalytic activation of CO_2 was observed under these conditions.

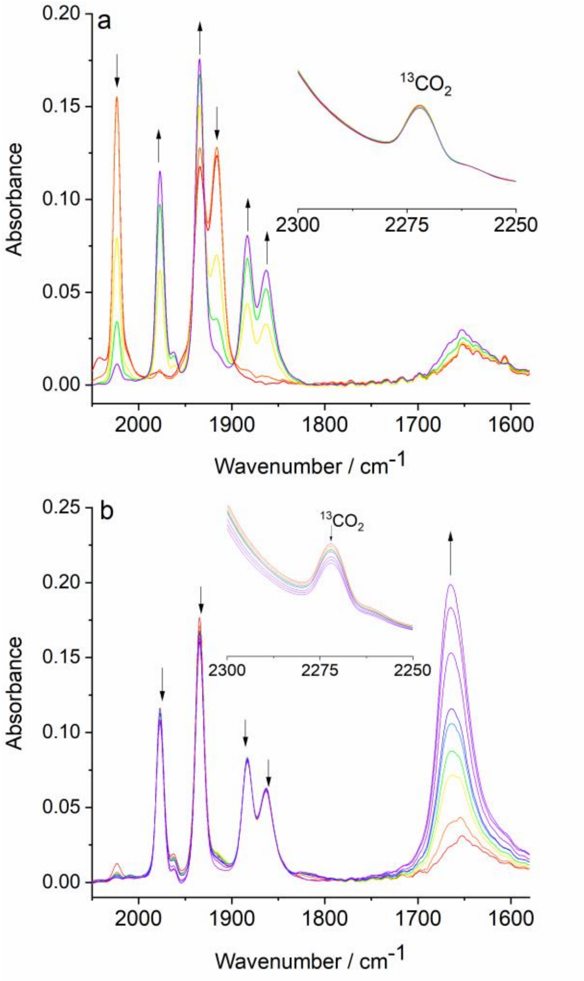

Figure SI-8. IR SEC monitoring of (a) the standard electrochemical reduction of [Mn(CO)$_3$(bipy)Br] (**1**) (↓) to [Mn(CO)$_3$(bipy)]$_2$ (↑) at R1, and (b) the dimer (↓) to [Mn(CO)$_3$(bipy)]$^-$ (↑) at R(D) (cf. Figure SI-5a), triggering electrocatalytic reduction of CO$_2$. Inset: the $^{13}CO_2$ satellite peak used as a reference. Conditions: CO$_2$-saturated THF/TBAH containing 5% MeOH, an OTTLE cell (Pt mesh cathode), *T* = 298 K.

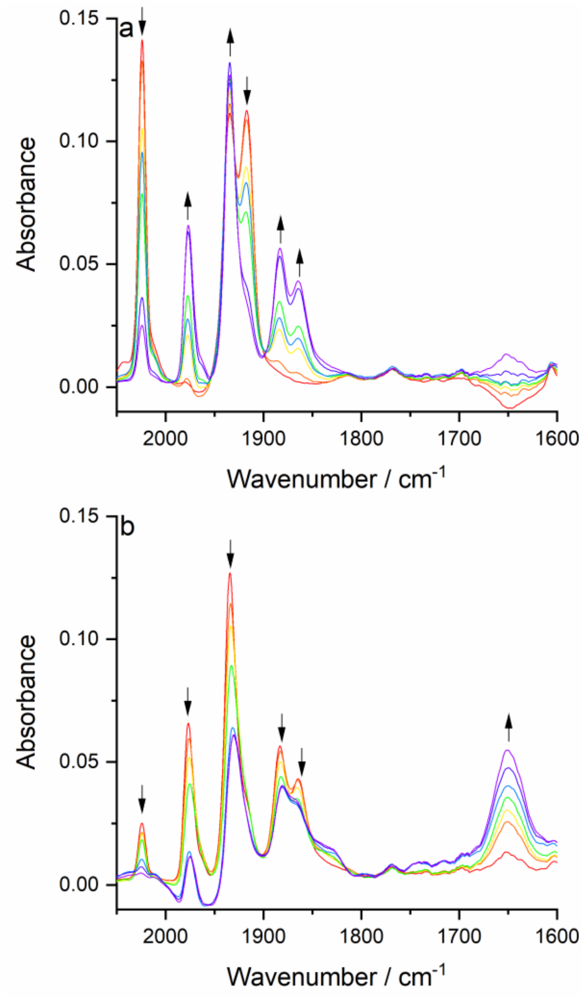

Figure SI-9. IR SEC monitoring of (a) the standard electrochemical reduction of [Mn(CO)$_3$(bipy)Br] (1) (↓) to [Mn(CO)$_3$(bipy)]$_2$ (↑) at R1, and (b) the dimer (↓) to [Mn(CO)$_3$(bipy)]$^-$ (↑) at R(D), triggering electrocatalytic reduction of $^{13}CO_2$. Conditions: $^{13}CO_2$-saturated THF/TBAH containing 5% TFE, an OTTLE cell (Pt mesh cathode), *T* = 298 K.

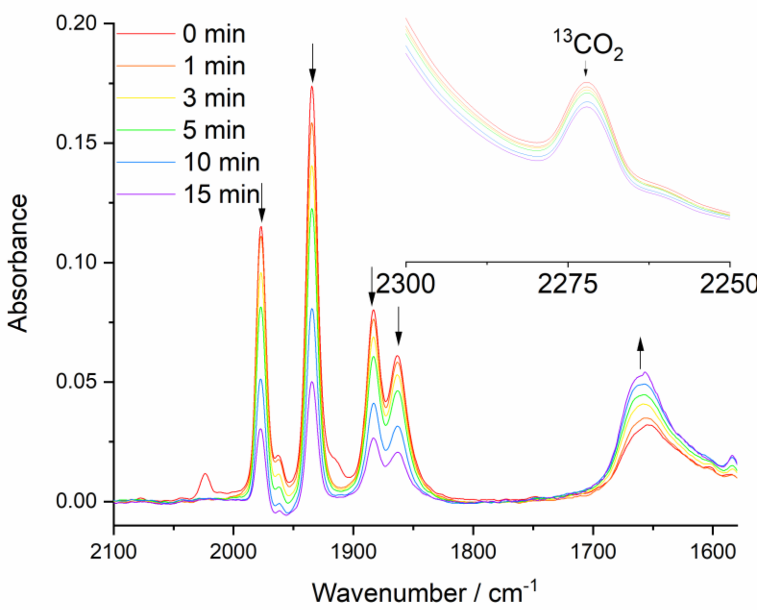

Figure SI-10. IR SEC monitoring of the photo-assisted electrochemical reduction of [Mn(CO)$_3$(bipy)]$_2$ (↓) pre-formed from **1** at R1, to [Mn(CO)$_3$(bipy)]$^-$ (↑) at the same cathodic potential (cf. Figure SI-5b), triggering electrocatalytic reduction of CO$_2$. Inset: the $^{13}CO_2$ satellite peak used as a reference. Conditions: CO$_2$-saturated THF/TBAH containing 5% MeOH, an OTTLE cell (Pt mesh cathode), λ_{exc} = 405 nm (irradiation times in minutes), *T* = 298 K.

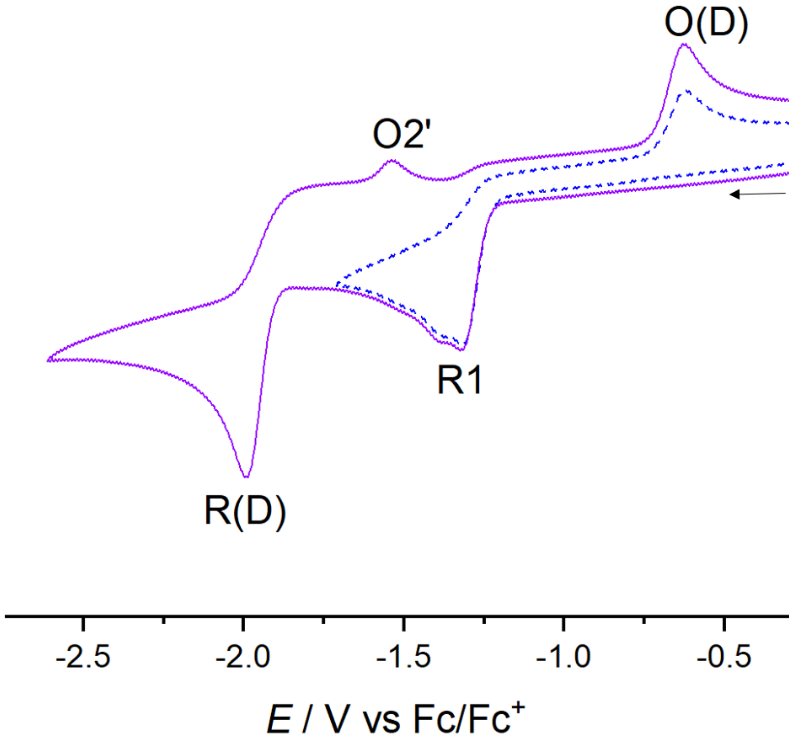

Figure SI-11. Cyclic voltammogram of [Mn(CO)$_3$(bipy)OTf)]. Conditions: Ar-saturated THF/TBAH, Pt microdisc, *v* = 100 mV s^{-1} , *T* = 298 K. Legend: R1 – reduction of the parent complex; R(D) and O(D) – reduction and oxidation of [Mn(CO)$_3$(bipy)]$_2$; O2' – oxidation of [Mn(CO)$_3$(bipy)]$^-$.

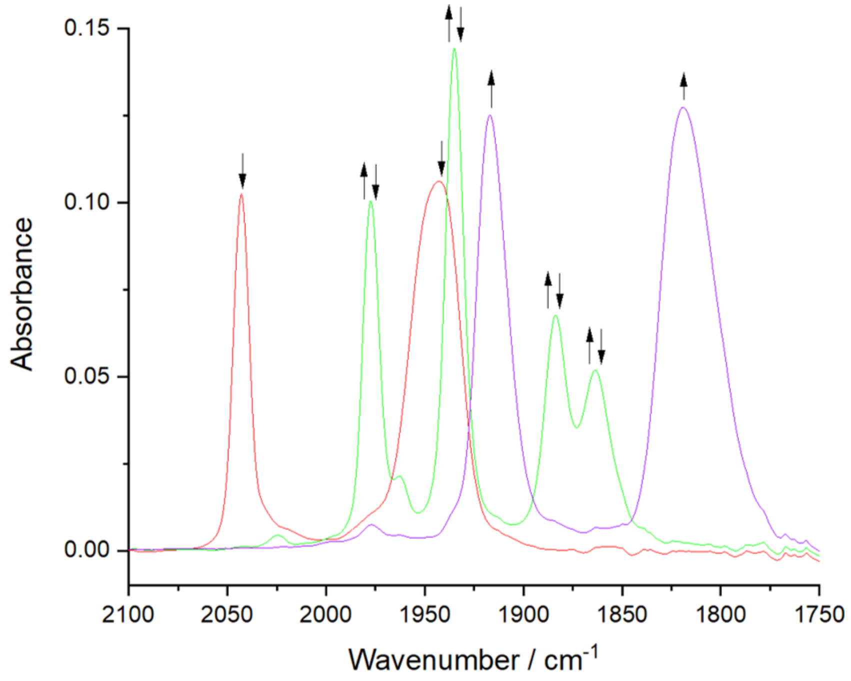

Figure SI-12. IR SEC monitoring of (a) the standard electrochemical reduction of [Mn(CO)$_3$(bipy)(OTf)] (1) (↓) to [Mn(CO)$_3$(bipy)]$_2$ (↑↓) at R1, and the dimer to [Mn(CO)$_3$(bipy)]$^-$ (↑) at R(D).

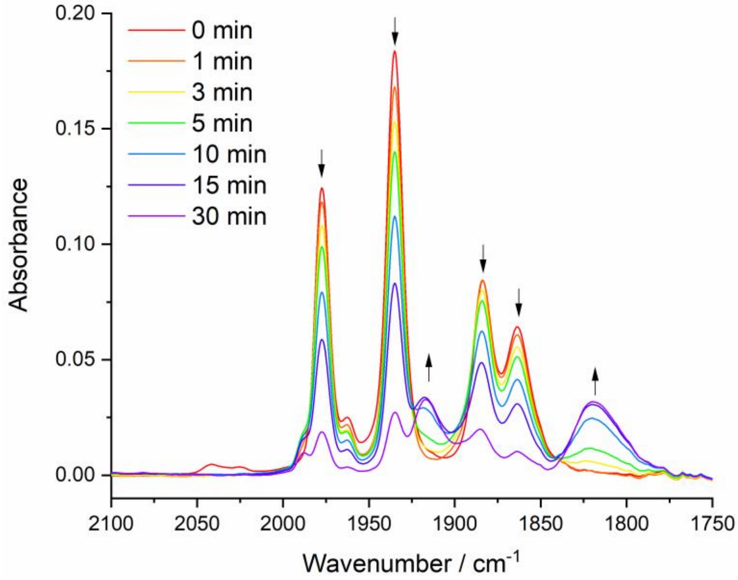

Figure SI-13. IR SEC monitoring of the photo-assisted electrochemical reduction of [Mn(CO)$_3$(bipy)(OTf)] (↓) at R2' which ultimately yields the 5-coordinate anion [Mn(CO)$_3$(bipy)]$^-$ (↑), following 405-nm irradiation of electrogenerated [Mn(CO)$_3$(bipy)]$_2$ (↓) over the course of several minutes. Some photodecarbonylation of the dimer has also taken place. Conditions: Ar-saturated THF/TBAH, an OTTLE cell (Pt mesh cathode), *T* = 298 K.

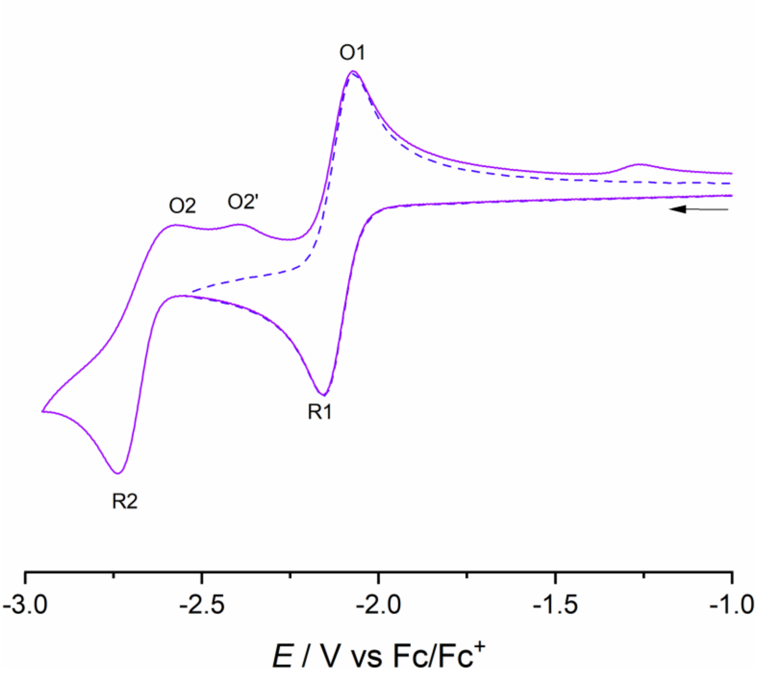

Figure SI-14. Cyclic voltammogram of [Mo(CO)$_4$(6,6'-dmbipy)]. Conditions: Ar-saturated THF/TBAH, Pt microdisc, *v* = 100 mV s^{-1}, *T* = 298 K.

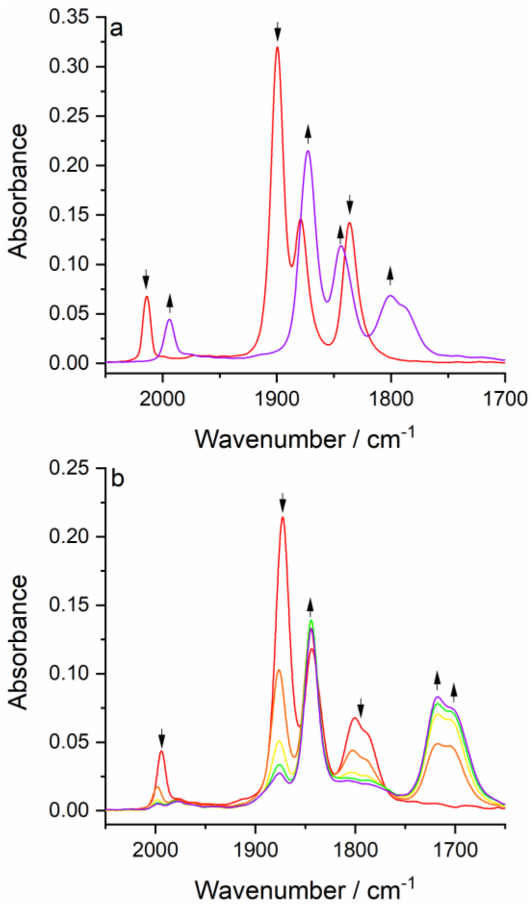

Figure SI-15 IR SEC monitoring of (a) reduction of [Mo(CO)$_4$(6,6'-dmbipy)] at R1 (see Figure SI-14) to [Mo(CO)$_4$(6,6'-dmbipy)]$^{\bullet-}$, and (b) reduction of the radical anion at R2 to 5-coordinate dianion, [Mo(CO)$_3$(6,6'-dmbipy)]$^{2-}$. Conditions: Ar-saturated THF/TBAH, OTTLE cell (Pt mesh cathode), *T* = 298 K.

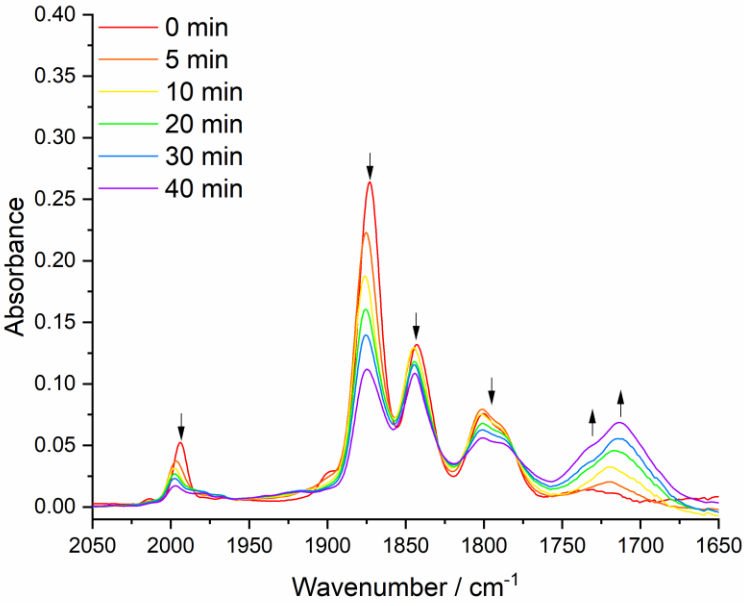

Figure SI-16 IR SEC monitoring of the photo-assisted electrochemical reduction of [Mo(CO)$_4$(6,6'-dmbipy)]$^{\bullet-}$ (↓) at R2' to the 5-coordinate dianion [Mo(CO)$_3$(6,6'-dmbipy)]$^{2-}$ (↑). Conditions: Ar-saturated THF/TBAH, OTTLE cell (Au mesh cathode), λ_{exc} = 365 nm (irradiation times in minutes), *T* = 298 K.

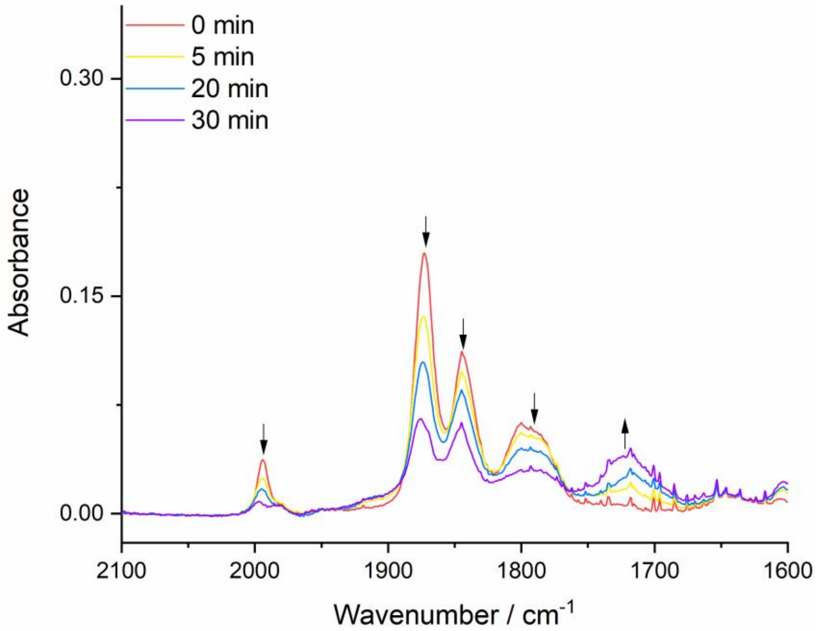

Figure SI-17 IR SEC monitoring of the photo-assisted electrochemical reduction of [Mo(CO)$_4$(6,6'-dmbipy)]$^{•–}$ (↓) at R2' to the 5-coordinate dianion [Mo(CO)$_3$(6,6'-dmbipy)]$^{2–}$ (↑). Conditions: Ar-saturated THF/TBAH, OTTLE cell (Cu mesh cathode), λ_{exc} = 365 nm (irradiation times in minutes), T = 298 K.

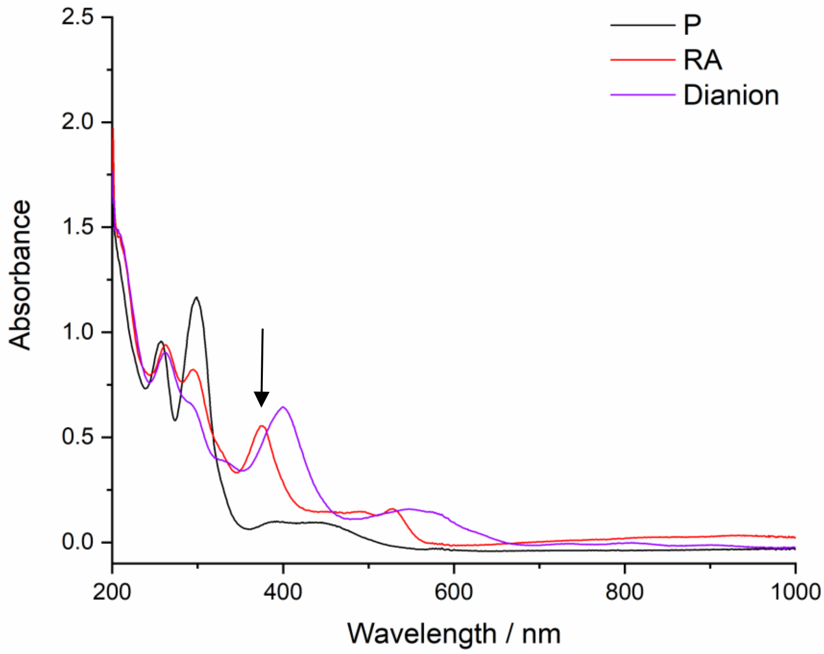

Figure SI-18. UV-vis absorption spectra of parent [Mo(CO)$_4$(6,6'-dmbipy)] (**2**, black), the radical anion [Mo(CO)$_4$(6,6'-dmbipy)]$^{•–}$ (red) and the 5-coordinate dianion [Mo(CO)$_3$(6,6'-dmbipy)]$^{2–}$ (purple). The arrow indicates the LED irradiation wavelength (365 nm) used to optically populate the MLCT excited state of the 1e$^–$ reduced radical anion. Conditions: Ar-saturated THF/TBAH, an OTTLE cell (Pt mesh cathode), T = 298 K.

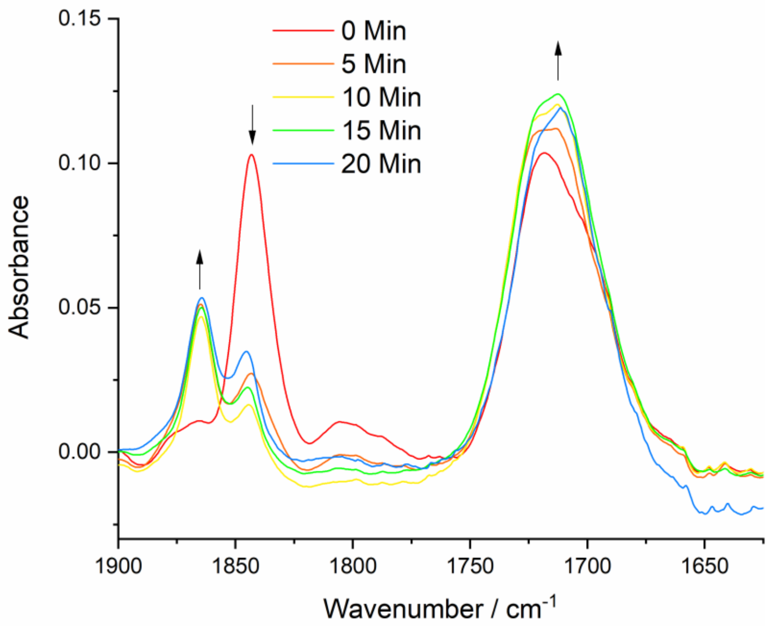

Figure SI-19 IR SEC monitoring of the photochemical (λ_{exc} = 365 nm) transformation of the 5-coordinate dianion, $[Mo(CO)_3(6,6'\text{-dmbipy})]^{2-}$ (↓), at R2 to an unknown tricarbonyl photoproduct (↑). Conditions: THF/TBAH, OTTLE cell (Pt mesh cathode), *T* = 298 K.

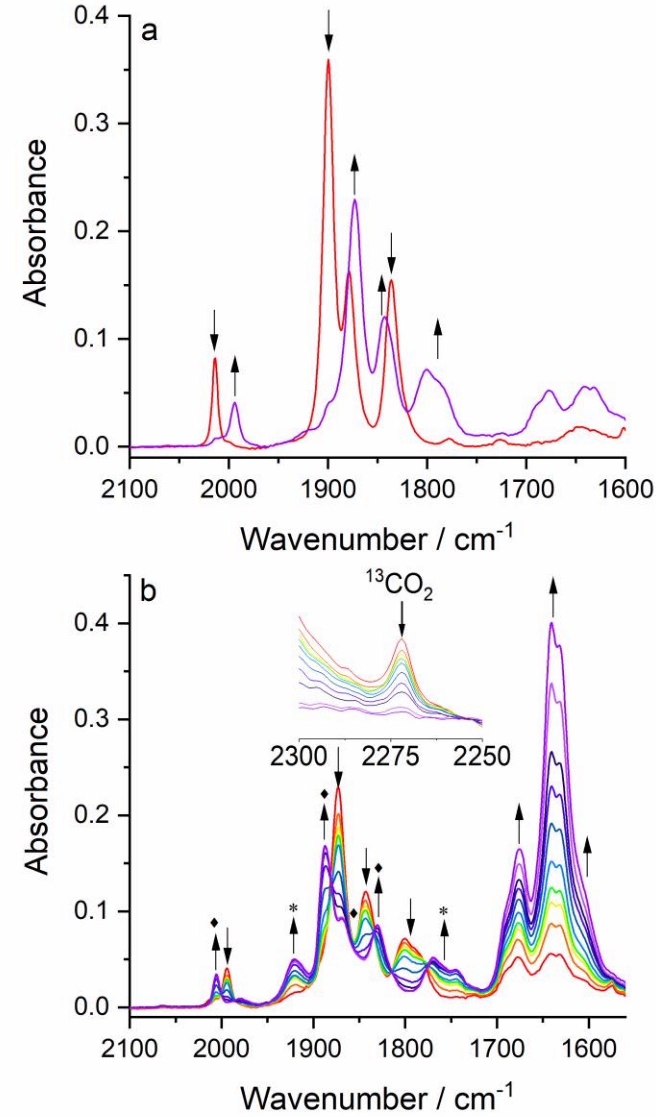

Figure SI-20 IR spectral monitoring of (a) the initial reduction of **2** at R1 producing the radical anion [Mo(CO)$_4$(6,6'-dmbipy)]]$^{\bullet-}$, and (b) the subsequent cathodic step at R2 triggering the catalytic conversion of CO_2 to CO and formate, with some amount of accompanying bicarbonate also formed. The labels ♦ denote an inactive tetracarbonyl complex, most likely an adduct of protonated anion [Mo(CO)$_4$(6,6'-dmbipy-H)]$^-$ with CO_2, replacing [Mo(CO)$_3$(6,6'-dmbipy)]$^{2-}$ (see Figure SI-15). Unassigned carbonyl side products are labelled with asterisk. Conditions: CO_2-saturated THF/TBAH, an OTTLE cell (Pt mesh cathode), *T* = 298 K.

References

[1] M. Bourrez, F. Molton, S. Chardon-Noblat, A. Deronzier, *Angew. Chemie Int. Ed.* **2011**, *50*, 9903–9906.

[2] E. Hevia, J. Pérez, L. Riera, V. Riera, D. Miguel, *Organometallics* **2002**, *21*, 1750–1752.

[3] J. O. Taylor, R. D. Leavey, F. Hartl, *ChemElectroChem* **2018**, *5*, 3155–3161.

[4] M. Krejčik, M. Daněk, F. Hartl, *J. Electroanal. Chem. Interfacial Electrochem.* **1991**, *317*, 179–187.